The EMBO Journal Vol.18 No.5 pp.1199–1213, 1999

A region of the *Yersinia pseudotuberculosis* invasin protein enhances integrin-mediated uptake into mammalian cells and promotes self-association

Petra Dersch and Ralph R.Isberg[1]

Department of Molecular Biology and Microbiology, Tufts University School of Medicine and Howard Hughes Medical Institute, 136 Harrison Avenue, Boston, MA 02111, USA

[1]Corresponding author
e-mail: risberg@opal.tufts.edu

Invasin allows efficient entry into mammalian cells by *Yersinia pseudotuberculosis*. It has been shown that the C-terminal 192 amino acids of invasin are essential for binding of β_1 integrin receptors and subsequent uptake. By analyzing the internalization of latex beads coated with invasin derivatives, an additional domain of invasin was shown to be required for efficient bacterial internalization. A monomeric derivative encompassing the C-terminal 197 amino acids was inefficient at promoting entry of latex beads, whereas dimerization of this derivative by antibody significantly increased uptake. By using the DNA-binding domain of λ repressor as a reporter for invasin self-interaction, we have demonstrated that a region of the invasin protein located N-terminal to the cell adhesion domain of invasin is able to self-associate. Chemical cross-linking studies of purified and surface-exposed invasin proteins, and the dominant-interfering effect of a non-functional invasin derivative are consistent with the presence of a self-association domain that is located within the region of invasin that enhances bacterial uptake. We conclude that interaction of homomultimeric invasin with multiple integrins establishes tight adherence and receptor clustering, thus providing a signal for internalization.

Keywords: bacterial uptake/integrin receptor clustering/invasin/protein–protein interaction/*Yersinia pseudotuberculosis*

Introduction

Adhesion and subsequent internalization within mammalian cells is a common strategy used by many pathogenic bacteria to establish a successful infectious niche (Finlay and Cossart, 1997). The Gram-negative bacterium *Yersinia pseudotuberculosis*, which causes systemic disease after initial gastrointestinal colonalization, translocates across the ileum into deeper host tissue. In animal infection models, the organism is internalized by M-cells which are intercalated into the epithelium overlaying ileal lymphoid follicles called Peyer's patches (Gruetzkau *et al*., 1990; Marra and Isberg, 1997). Efficient translocation into the Peyer's patch requires the bacterial protein invasin (Pepe *et al.*, 1995; Marra and Isberg, 1997). Cellular internalization of *Y.pseudotuberculosis* can be reproduced *in vitro* using a number of normally non-phagocytic cultured cell lines and has been used to identify critical components involved in target cell adherence and penetration (Devenish and Schiemann, 1981; Isberg, 1991). The most efficient factor that promotes internalization in culture is invasin. This 986 amino acid (108 kDa) bacterial outer membrane protein is encoded by the chromosomal *inv* gene which, when expressed in normally non-adherent laboratory *Escherichia coli* strains, confers the ability to penetrate mammalian cells (Isberg and Falkow, 1985; Isberg *et al*., 1987). Homologous invasin proteins have been found in other pathogenic *Yersinia* species (Miller and Falkow, 1988; Simonet *et al*., 1996) and are highly similar to a family of proteins called intimins, involved in attachment of a variety of related Gram-negative enteric pathogens to host cells (Jerse *et al*., 1990; Schauer and Falkow, 1993; Frankel *et al*., 1994).

Invasin promotes entry into eukaryotic cells by binding to at least five different members of the β_1 integrin receptor superfamily (Isberg and Leong, 1990; Krukonis and Isberg, 1997). Integrins are αβ heterodimeric proteins found on the surface of most mammalian cells and are involved in a wide variety of adhesive functions, such as cell–cell interaction, cell migration, differentiation and adhesion. Members of this receptor family are able to bind extracellular matrix proteins (ECMs) as well as cytoskeletal components, thus providing a sophisticated communication system between the extracellular environment and the intracellular cytoskeleton (Hynes, 1992; Clark and Brugge, 1995).

Analysis of truncated derivatives has shown that a region corresponding to the extreme C-terminal 192 amino acids of invasin is sufficient to promote integrin-dependent cell adhesion and is necessary for both bacterial attachment and internalization by target cells (Figure 1A; Leong *et al*., 1990, 1995; Rankin *et al*., 1992). Invasin derivatives containing C-terminal fragments shorter than 192 amino acids are unable to promote binding and uptake when immobilized by antibody on the surface of *Staphylococcus aureus* (Rankin *et al*., 1992; Saltman *et al*., 1996). One striking characteristic of the invasin C-terminus is the presence of an intramolecular disulfide bond between residues 907 and 982 that appears to be required for integrin recognition (Leong and Isberg, 1993; Leong *et al*., 1993). Analysis of entry-deficient mutants indicates that the single most critical residue for bacterial penetration is an aspartate at position 911 (Leong *et al*., 1995; Saltman *et al*., 1996). Substitutions at this residue render bacteria unable to enter into mammalian cells (Leong *et al*., 1995). D911 seems to have a cell adhesion function similar to that of the aspartate residue in the RGD-containing motif of natural integrin ligands (Ruoslahti and Pierschbacher, 1987). As is true of fibronectin, a second region of the protein ~100 amino acids N-terminal to this critical site also has residues that contribute to receptor binding (Obara *et al.*, 1988; Saltman *et al*., 1996).

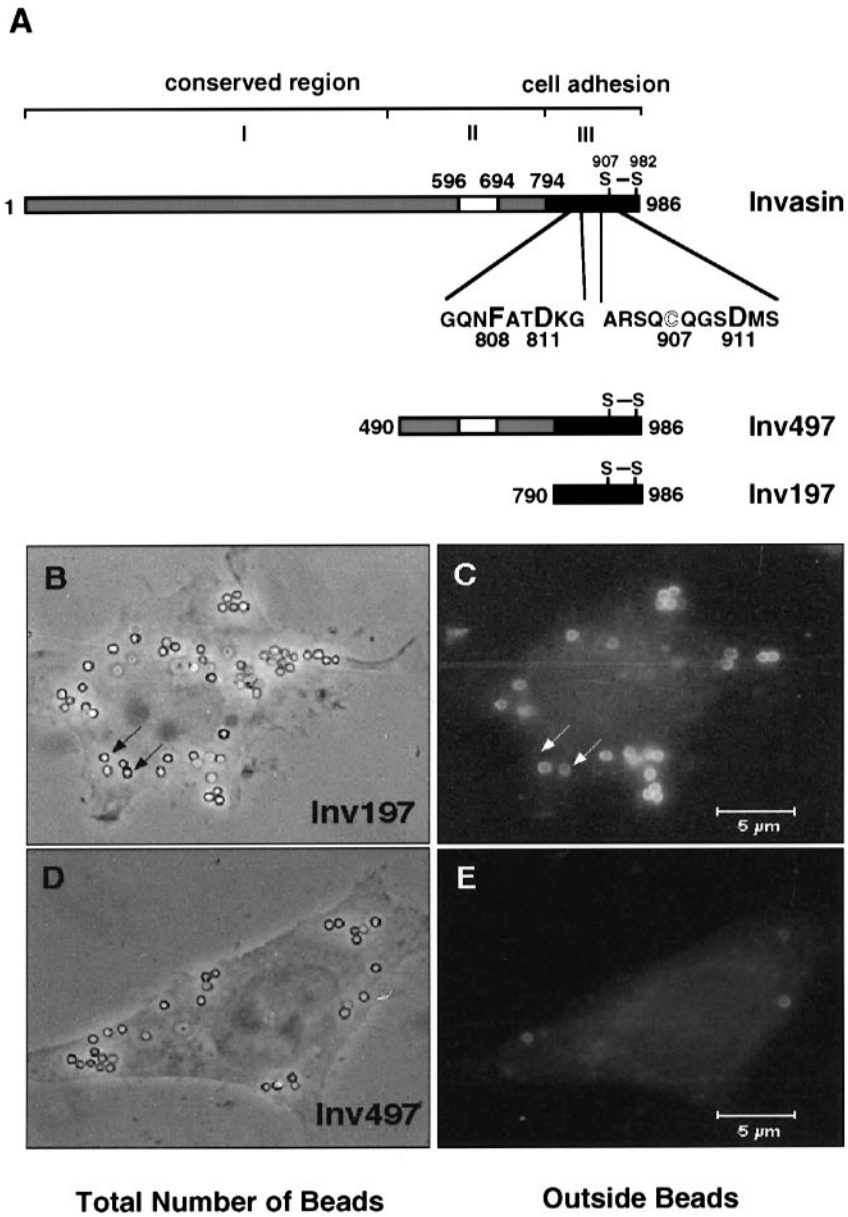

Fig. 1. (**A**) The structure of the *Y.pseudotuberculosis* invasin protein. The highly conserved module I and the less conserved module II are shown. Module II has an insertion (white) which is unique to the *Y.pseudotuberculosis* protein (see below and Figure 8). The cell adhesion domain III is symbolized by a black box. The C-terminal disulfide bond is indicated, and two amino acid regions including the crucial amino acids F808, D811 and D911 involved in uptake are noted. The MBP fusion derivatives, MBP–Inv197 and MBP–Inv497, comprising the C-terminal 197 and 497 amino acids of invasin, respectively, are shown schematically below. The junction residues of the invasin proteins are indicated. For experiments in which invasin was used in the absence of fusion sequences, each MBP–Inv derivative was cleaved with factor Xa and the invasin fragment was purified, as described (Materials and methods). (**B**–**E**) Fluorescence challenge uptake assay of latex beads coated with different invasin derivatives. One milligram per milliter Inv197 (B and C) and Inv497 protein (D and E) cleaved from MBP fusion derivatives and purified (Materials and methods) were used to coat 1 μm latex beads (>100 000 molecules/bead). The beads (5×10^6) were blocked as described, incubated with HEp-2 cells for 1 h (Materials and methods), probed with FITC–streptavidin and visualized by immunofluorescence (C and E). The total number of inside and outside beads that were associated with HEp-2 cells were visualized and counted microscopically by phase contrast (B and D). The right arrow marks the position of an adherent, the left arrow marks an intracellular bead. Bar = 5 μm.

Although the interaction of invasin with its receptors has been characterized in detail, less is known regarding the mechanism by which invasin triggers integrin-mediated bacterial uptake. Efficient entry requires tight binding of the bacterium to its host cell, which results in the extension of tight-fitting pseudopods around individual bacteria, each of which is internalized into a membrane-bound phagosome (Isberg, 1989; Tran Van Nhieu *et al.*, 1996). This zipper-like process morphologically resembles conventional phagocytosis of complement-coated particles by professional activated phagocytes (Swanson and Baer, 1995). Invasin-mediated entry is somewhat different from natural ligand binding, as mere attachment of a substrate to β_1 integrins is usually not sufficient to trigger the signal transduction pathway necessary for uptake. For example, bacteria coated with fibronectin adhere to host cells, yet they are internalized inefficiently, possibly because fibronectin binds with a lower affinity than does invasin to the integrin receptor (Van de Water *et al.*, 1983; Hook *et al.*, 1989; Tran Van Nhieu and Isberg, 1993a,b; Yang

and Isberg, 1993). Thus, it has been assumed that the sole unique feature of invasin that ensures its ability to promote bacterial uptake is its high affinity binding of receptor.

In this study, we investigated invasin-mediated uptake of a variety of invasin derivatives and report the identification and analysis of a region of the protein that enhances bacterial uptake. We present several lines of evidence that a domain within this region can promote self-association. Inability to self-associate is strongly correlated with an inability to promote efficient uptake of particles that specifically adhere to integrin receptors.

Results

Identification of an 'uptake enhancer' within invasin

To investigate invasin-dependent entry in the absence of other bacterial factors, uptake of invasin-coated latex beads was analyzed. Serial dilutions of two purified derivatives carrying the C-terminal 497 and 197 amino acids of invasin (Inv497 and Inv197, Figure 1A; Materials and methods) were coated onto 1.1 μm inert latex beads, assayed for the number of molecules bound per bead and used to challenge HEp-2 cells (Materials and methods). After a 1 h challenge of beads coated with a large excess of protein (>100 000 molecules per bead), internalized and extracellular beads were identified and quantitated by immunofluorescence microscopy. Control beads coated with bovine serum albumin (BSA) or maltose-binding protein (MBP) rarely were found to be associated with HEp-2 cells under the conditions used for the assay (<0.1%). More than 90% of Inv197- and Inv497-coated beads observed were associated with HEp-2cells, and a large number of bound beads were found to be internalized (Figure 1B–E). Control beads coated by fibronectin or polylysine were bound efficiently (80 and 60% of input, respectively) but, in marked contrast, only a few of these beads were found to be internalized (<1%, data not shown).

The uptake efficiency of the beads coated with Inv497 protein was significantly higher than that of Inv197 (Figure 1B–E) and was comparable to that seen with *Y.pseudotuberculosis* (24%; Marra and Isberg, 1997). Both invasin derivatives stimulated binding and uptake of beads in a concentration-dependent manner; however, at all coating concentrations, Inv497-coated beads were somewhat more adherent (Figure 2A) and internalized far more efficiently than beads coated with the Inv197 derivative (Figure 2B). The difference in uptake efficiency of cell-bound Inv497- and Inv197-coated beads was especially pronounced at low coating concentrations. For instance, ~2000 Inv497 molecules were sufficient to mediate uptake of 20% of bound beads, whereas 10 times more Inv197 molecules were necessary to obtain the same efficiency of uptake. Moreover, particles coated with <2000 molecules of Inv197 were unable to promote cellular penetration. The effects observed were highly concentration dependent, as increasing the number of Inv197 molecules from 4×10^3/bead to 1×10^5/bead had little effect on the number of associated beads, but increased the internalization efficiency of bound beads 10-fold (Figure 2). These results indicated the presence of a region that enhances uptake in the Inv497 protein and is absent from the Inv197 derivative.

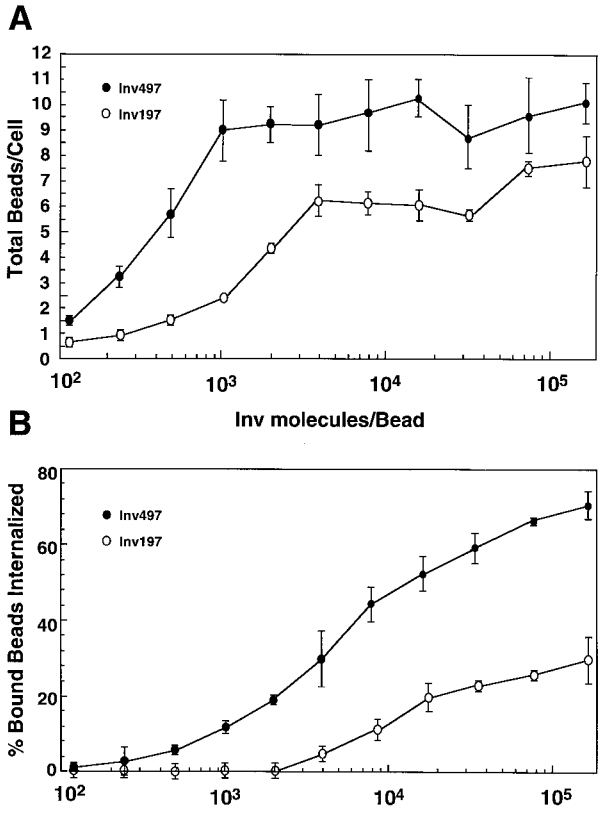

Fig. 2. Binding and entry efficiency of latex beads coated with different invasin derivatives. A total of 5×10^6 beads coated with Inv197 (○) and Inv497 (●) as described (Materials and methods) were used to challenge HEp-2 cells, and surface-bound beads were visualized by immunofluorescence microscopy. The total number of cell-associated beads was visualized and counted microscopically with phase contrast (**A**) and the percentage of adherent beads internalized per cell is shown in (**B**).

The Inv497 derivative behaves in solution as if it has a large radius

Based on the concentration effects, we predicted that the low efficiency uptake of adherent beads coated by Inv197 may be due to an inability of the protein to form higher order complexes of invasin subunits in the bacterial outer membrane. A series of experiments was performed to determine if the invasin protein is able to interact with itself. To analyze the relative Stokes radius of Inv497 and Inv197, the proteins were size-fractionated on a Superose 6 column (Materials and methods). No Inv497 protein was detected in the elution volume containing globular proteins of predicted mol. wt <60 kDa, where monomeric Inv497 with an apparent molecular mass of 52.6 kDa would be expected to fractionate (Figure 3A). Peak elution of Inv497 occurred in a region of the column predicted to contain spherical proteins of ~200 kDa (Figure 3A). This indicates that the protein is either multimeric, has an elongated structure or both. In contrast, purified Inv197 protein fractionated with a peak elution consistent with a 20 kDa species, indicating that this derivative is monomeric (Figure 3A). Sedimentation equilibrium data, however, gave a contrasting result. For the most dilute initial concentration of protein analyzed, Inv497 sedimented as would be expected for a monomeric derivative with an apparent mol. wt of 51.4 kDa (Table I). The behavior of this protein, however, was highly non-ideal. Sedimentation

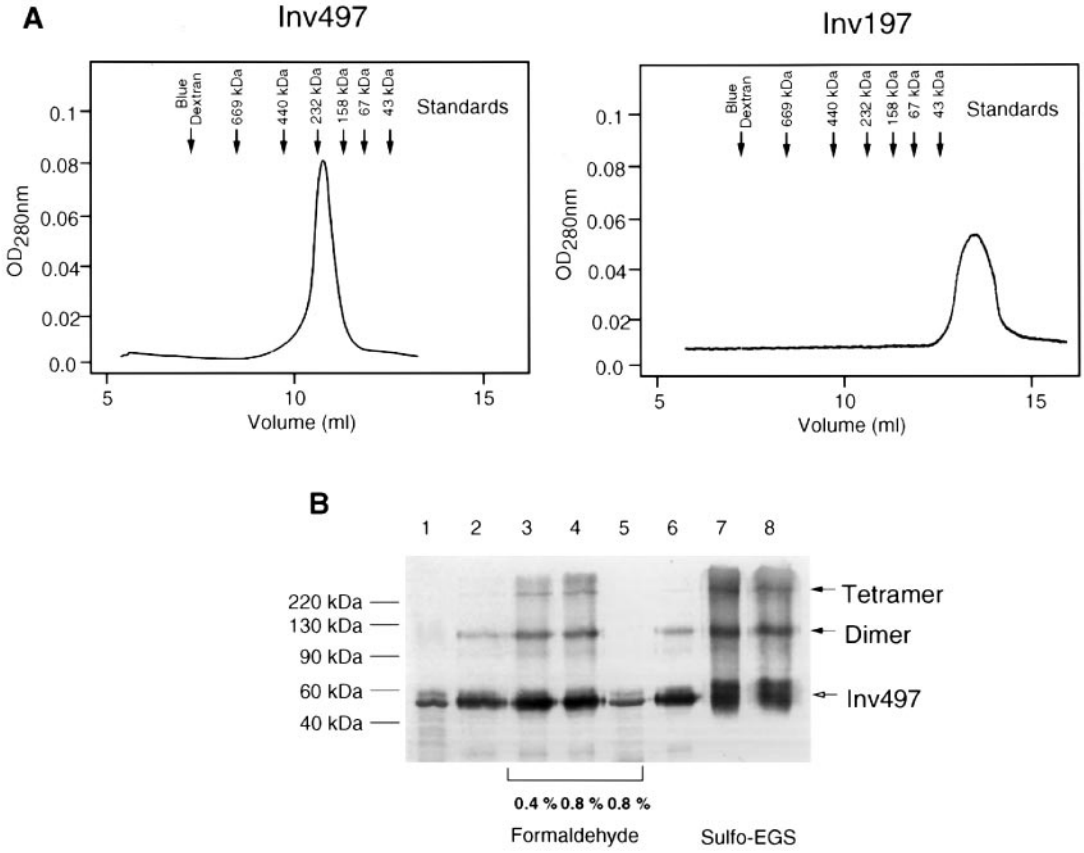

Fig. 3. (**A**) Size fractionation of purified Inv197 and Inv497. A 200 μg aliquot of Inv497 and Inv197 proteins cleaved from MBP–Inv derivative by factor Xa and purified from MBP was size-separated using a Superose 6 column. The elution profile of both proteins is shown, monitored by their absorbance at 280 nm. Marker proteins are as described in the Materials and methods. The peak fractions of these marker proteins and the void sample (Blue Dextran 2000) are indicated by arrows. (**B**) *In vitro* cross-linking of purified Inv497. A 2 μg aliquot of purified Inv497 was cross-linked for 30 min at room temperature using increasing amounts of formaldehyde or Sulfo-EGS. Samples were added to SDS sample buffer, and not heated unless otherwise indicated, before loading on a 12% SDS–polyacrylamide gel. Shown is an immunoblot using anti-invasin mAb3A2. Sample heated to 100°C (lane 1), incubated in the absence of heating without cross-linker (lanes 2 and 6) and with 0.4% (lane 3) or 0.8% (lane 4) formaldehyde; treated with 0.8% formaladehyde, then boiled for 20 min (lane 5), treated with Sulfo-EGS at 1 mM (lane 7) and 2 mM (lane 8) final concentration. The molecular mass standard is shown on the left, cross-linked complexes are indicated by closed arrows, and the position of Inv497 and Inv197 is indicated by an open arrow.

Table I. Sedimentation equilibrium analysis of the Inv497 fragment

Initial concentration (mg/ml)[a]	R.p.m.[b]	Apparent mol. wt
0.055	1.3×10^4	51.4
0.60	1.3×10^4	48.3
1.5	1.3×10^4	43.4
1.5	1.0×10^4	44.8

[a]Protein was adjusted to the noted initial concentration in 20 mM Tris–HCl (pH 8.0), 100 mM NaCl and subjected to sedimentation equilibrium analysis performed in the identical buffer with a Beckman optima XL-A analytical ultracentrifuge.
[b]Revolutions per minute of sedimentation run. All runs were performed for 6 h.
[c]Molecular weights were determined by non-linear least squares fit of the equilibrium gradient, plotting absorbance (*A*) versus radius in rotor (*r*), for each solution, and using the model of single ideal species with the manufacturer's software. For the solution of the highest initial concentration, the plot of the error indicated deviation from ideality, which is also apparent from the plot of ln(*A*) versus r^2.

analysis of protein analyzed at a relatively low initial protein concentration (1.5 mg/ml) gave results that strongly deviated from the expected mol. wt of 52 600 (Table I). In addition, the plot of ln (concentration) versus r^2 was non-linear, indicating non-ideal behavior of the protein (data not shown). These results may be due to charge effects, an elongated structure of the protein or self-association during sedimentation.

In vitro and in vivo cross-linking of invasin identifies invasin oligomers

As two physical techniques gave inconsistent results, the possibility of physical interaction between invasin monomers dependent on a region of the protein found in Inv497 but not in Inv197 was investigated further. Chemical cross-linking experiments of Inv497 using formaldehyde, BS^3 and Sulfo-EGS generated two dominant species with apparent molecular masses of 120 kDa (35% of total Inv497 antigen) and 240 kDa (8% of total Inv497 antigen) for all cross-linking agents used (Figure 3B, data for BS^3 not shown). The difference in molecular mass between the two identified species and the Inv497 monomer (52.6 kDa) was consistent with the formation of both homodimeric and homotetrameric cross-linking products. Formaldehyde resulted in cross-links that were able to be disrupted by boiling and liberated the unaltered individual cross-link component (Figure 3B, lane 5). It should be noted that even in the absence of cross-linking

agents, unboiled samples containing SDS gave a small amount of the predicted dimeric form of the Inv497 molecule detectable on Western blots (Figure 3B, lanes 2 and 6). The same cross-linking treatment had no effect on the Inv197 protein and did not lead to the formation of higher molecular weight products under any conditions (data not shown).

To determine if the interaction between invasin monomers observed with the purified Inv497 occurs with intact invasin in the bacterial outer membrane, *in vivo* cross-linking experiments were performed. An *E.coli inv*$^+$ strain was subjected to cross-linking by formaldehyde, BS^3 or Sulfo-EGS at 0°C; extracts were prepared, and the results were analyzed by gel electrophoresis and immunoblotting. In all extracts, the 108 kDa invasin polypeptide and several species lacking various amounts of the N-terminus were detected, as noted previously (Figure 4B, lane 2; Isberg *et al*., 1987; Isberg and Leong, 1988). In extracts from intact bacteria subjected to cross-linking by formaldehyde, two novel bands appeared that were of apparent molecular weights greater than the wild-type invasin monomer (Figure 4B, lanes 3 and 4). Parallel experiments with cells lacking the *inv* gene showed no reaction with the anti-invasin monoclonal antibody (Figure 4B, lane 1). The largest cross-linking product had an apparent molecular mass of ~400 kDa or higher, consistent with that of an invasin tetramer. Its weak intensity may be explained by difficulty in the electrophoretic transfer of higher molecular weight complexes. The smaller of the two cross-linked bands had a mol. wt of ~140 kDa, and its appearance was accompanied by the disappearence of the truncated 70 kDa invasin product upon addition of increasing amounts of cross-linking reagents (Figure 4C, lanes 3 and 4). This is consistent with the 140 kDa cross-reactive species being the dimeric form of the 70 kDa species. Identical results were obtained with two membrane-impermeant high molecular weight cross-linkers, Sulfo-EGS (Figure 4C) and BS^3 (Figure 4D), which were used to exclude the possibility of cross-linking of any potential intracellular precursors of invasin.

To investigate the region of invasin responsible for cross-linking, the identical experiments were performed on bacteria expressing the internal deletions InvΔKpn and InvΔHpa, lacking residues 608–794 and 804–850, respectively (Figure 4A). Both derivatives are surface exposed at almost the same levels as wild-type invasin (see Table II). In the case of InvΔHpa (Figure 4D, lanes 4–6), bands of a higher molecular mass corresponding to a tetrameric form of the *Hpa*I deletion product and a dimer of the shorter truncated product were detected. Interestingly, multimer formation of the InvΔHpa protein seemed to be somewhat more efficient than that of the wild-type, with almost complete disappearance of the full-length 104 kDa product (Figure 4D, lanes 5 and 6). In contrast, no cross-linked product was detected with the InvΔKpn deletion product (Figure 4D, lanes 7–9), consistent with a loss of the capacity for protein–protein interaction. These results indicate that a region upstream from the C-terminal cell-binding region is required for cross-linking, which is consistent with the cross-linking data on the purified Inv 497 and Inv197 derivatives.

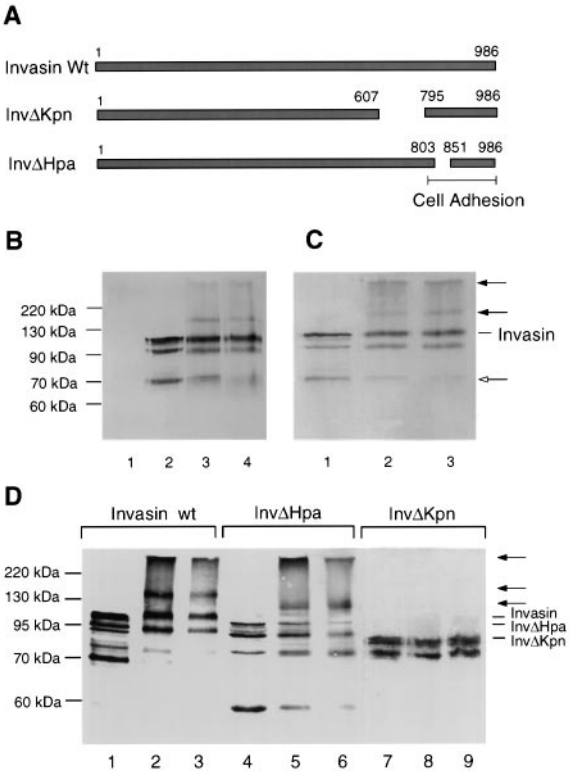

Fig. 4. *In vivo* cross-linking of wild-type and deletion derivatives of invasin. (**A**) The structure of the *Y.pseudotuberculosis* invasin protein and the deletion derivatives InvΔHpa and InvΔKpn are shown schematically. The amino acids of the deletion junctions are indicated. (B–D) Immunoblots of bacteria expressing wild-type or invasin deletion derivatives cross-linked with formaldehyde (**B**), Sulfo-EGS (**C**) or BS^3 (**D**). (B): XL1blue (pBR322) (lane 1), XL1blue [pRI203 (*inv*$^+$)] incubated with 0% (lane 2); 0.4% (lane 3) and 0.8% (lane 4) formaldehyde; (**C**): XL1blue [pRI203 (*inv*$^+$)] cross-linked by 0 mM (lane 1), 1 mM (lane 2) and 2 mM (lane 3) Sulfo-EGS; (D): BS^3 cross-linking of XL1blue harboring pRI203 (*inv*$^+$) (lanes 1–3), pPD214 (*invΔHpa*I) (lanes 3–4) and pRI207 (*invΔKpn*I) (lanes 7–9). BS^3 was used at 0 mM (lanes 1, 4 and 7), 1 mM (lanes 2, 5 and 8) and 2 mM (lanes 3, 6 and 9). Cross-linking and blocking were performed at 0°C as described (Materials and methods). The wild-type invasin protein and the InvΔHpa derivative were visualized using monoclonal antibody mAb2A9, and the InvΔKpn protein was detected with monoclonal antibody mAb3A2. Invasin or deletion derivatives are marked; cross-linked products are indicated by closed arrows. The position of the truncated 70 kDa invasin product is indicated by an open arrow.

A binding- and uptake-deficient mutation in Asp911 of invasin confers a dominant-negative phenotype

Several residues of invasin have been identified that are necessary for efficient cellular penetration (Leong and Isberg, 1993; Leong *et al*., 1995; Saltman *et al*., 1996). The most critical residue for cell attachment and entry is Asp911 of the C-terminal cell attachment domain (Figure 1A). Changes in this residue lower bacterial penetration to background levels and almost entirely abrogate cell attachment, such that only the most conservative mutation D911E retains detectable cell attachment activity (Leong *et al*., 1990, 1995). To assess further the ability of invasin to form multimers *in vivo*, we investigated the effects of the internal deletions, InvΔHpa and InvΔK, and three Asp911 point mutations on bacterial entry when co-expressed with wild-type invasin.

Escherichia coli strains harboring high copy number

Table II. Dominant-negative phenotype of cell binding and adhesion mutations InvD911A and D911T

Plasmid	Protein produced[a]	Entry efficiency[b]	Surface expression[c]	Cell binding[d]
Select-2	None	<0.001	<0.001	−
pSelect-2-8	wt invasin	1.0	1.0	+++
pJL272	wt invasin	1.0	1.1	+++
pJL272-D911E	InvD911E	<0.001	0.99	+
pSelect-2-8-D911A	InvD911A	<0.001	1.01	−
pJL316-D911T	InvD911T	<0.005	0.99	−
pPD214	InvΔHpaI	<0.001	0.82	−
pRI207	InvΔKpnI	0.04	0.89	++
λgt11*inv*$^+$/pSelect-2	wt invasin	1.0	0.95	+++
λgt11*inv*$^+$/pSelect-2–8	wt invasin/wt invasin	1.2	1.2	+++
λgt11*inv*$^+$/pJL272	wt invasin/wt invasin	1.2	1.2	+++
λgt11*inv*$^+$/pJL272-D911E	wt invasin/InvD911E	0.89	1.0	+++
λgt11*inv*$^+$/pSelect-2-8D911A	wt invasin/InvD911A	0.05	1.2	+++
λgt11*inv*$^+$/pJL316D911T	wt invasin/InvD911T	0.5	1.4	+++
λgt11*inv*$^+$/pPD214	wt invasin/InvΔHpaI	0.82	0.89	+++
λgt11*inv*$^+$/pRI207	wt invasin/InvΔKpnI	0.95	0.85	+++

[a]Protein was expressed in *E.coli* strain XAcSu6 or XAcSu6(λgt11*inv*Δ8–15) harboring the denoted plasmid. Point mutations are indicated by single letter amino acid designation and numbers indicate the invasin residue.
[b]Entry efficiency was calculated as the percentage of bacteria that survive gentamicin treatment relative to wild-type control and is the mean of three determinations (Leong *et al.*, 1995).
[c]Surface exposure was determined using quantitative immunoprobing with mAb3A2, which recognizes an epitope between amino acids 795 and 986 of invasin (Leong *et al.*, 1990). Values shown are expressed relative to the absorbance (A_{595}) obtained with *E.coli* XAcSu6/pSelect-2-8, defined as 1.00, and are the mean of three determinations (see Materials and methods).
[d]Cell-binding activity assays were performed as described previously (Leong *et al.*, 1995). +++, activity indistinguishable from wild-type invasin; ++, activity significantly less than for wild-type invasin; +, activity detectable only when high concentrations of HEp-2 cells (>2×10^6/ml) were used; –, undetectable cell-binding activity.

plasmids with the *inv* wild-type or mutated derivatives in the presence or absence of a chromosomal *inv* gene were tested for cell entry into cultured HEp-2 cells (Table II). Mutated invasin derivatives tested in the absence of the chromosomal *inv* gene showed significantly decreased cell binding and bacterial internalization efficiencies relative to the chromosomal *inv*$^+$ wild-type control (Table II). Notably, the internal *inv*Δ*Kpn* deletion product which was unable to mediate invasin interaction in the cross-linking experiments (Figure 4D) exhibited only 4% of wild-type uptake efficiency, although it showed significant cell adhesion. Consistent with previous observations (Leong *et al.*, 1995), strains expressing the mutated derivatives InvD911A, E or T lost activity completely and promoted neither cell binding nor entry.

When transformed into the strain XAcSu6(λgt11-*inv*8-15) harboring a chromosomal *inv* gene, the plasmid-encoded InvD911A or InvD911T derivatives showed significant dominant-interfering effects on internalization (Table II). The InvD911T mutant strain was 50% less efficient in bacterial uptake, while InvD911A reduced internalization efficiency to ~5% of wild-type. Most importantly, neither point mutation interfered with cell attachment. In contrast, mutations that prevent invasin interaction (*inv*Δ*Kpn*) or have a less severe effect on cell uptake (D911E) did not interfere with bacterial internalization by wild-type invasin (Table II). Surprisingly, the *inv*Δ*Hpa* deletion product did not confer a dominant-interfering phenotype. This might be explained by the efficient InvΔHpa self-association, observed in the cross-linking experiments (Figure 4D), which may reduce the overall amount of non-functional heteromultimeric complexes. Alternatively, the deletion product may result in a protein structure that is unable to associate with wild-type invasin.

The interfering effect of the D911A mutation was also found in *Y.pseudotuberculosis*, although the uptake defect was less pronounced than that seen with *E.coli* (data not shown). In *Yersinia*, a lower plasmid copy number may explain the less drastic effect of the D911A mutation.

A region of invasin promotes protein–protein interaction

To map the region in invasin responsible for protein–protein interaction, the one-hybrid λ repressor system was used (Hu, 1990). This allows testing of potential multimerization domains fused to the monomeric DNA-binding domain (cI_N) of λ repressor. Only multimeric λ repressor binds strongly to the λP_R operator and efficiently represses transcription of a λP_R-*lacZ* reporter gene. Derivatives were constructed in which the DNA-binding domain of cI was fused to the C-terminal 478 and 202 amino acids of invasin (cI_N–Inv478 and cI_N–Inv202). Repression of transcription by the cI_N–Inv fusion proteins was compared with: (i) the properties of intact λ repressor (cI); (ii) a cI-leucine zipper chimera (cI_N–GCN4) that behaves similarly to intact λ repressor (Hu, 1990); (iii) the DNA-binding domain of cI alone (cI_N); and (iv) the cI-leucine zipper chimera interrupted by truncated *lacZ* sequences (cI_N–LacZ′). All chimeric proteins were readily detected on SDS–polyacrylamide gels of cell extracts under inducing conditions, and their steady-state levels were essentially identical under non-inducing conditions, based on Western blot analysis (data not shown). Wild-type λ repressor and the cI_N–GCN4 chimera yielded 86 and 88% repression of λP_R, respectively, whereas the monomeric cI N-terminus showed only 41% repression, as expected (Figure 5, Materials and methods). Cells expressing the cI_N–Inv478 protein exhibited 84% repression of λP_R, essentially identical to the cI_N–GCN4

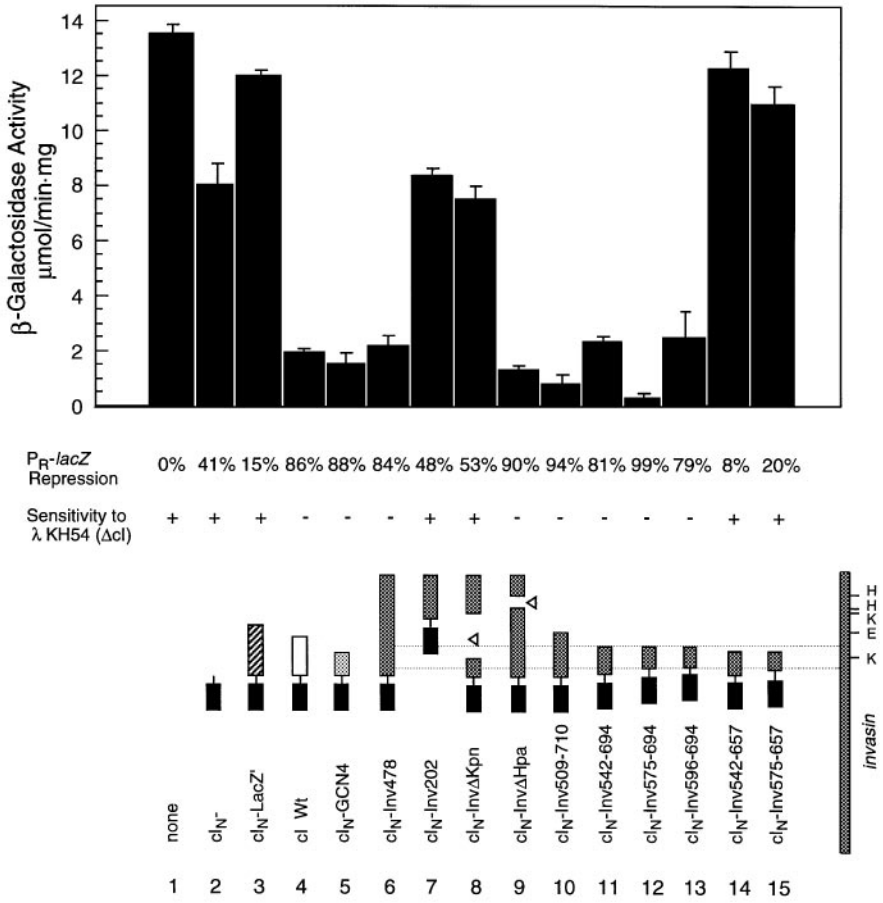

Fig. 5. Repressor activity of cI_N–Inv chimeric proteins. Repression and sensitivity to phage KH54(ΔcI) were measured as described in the Materials and methods. The efficiency of KH54(ΔcI) plating represents sensitivity to a phage lysate of 10^9 phages/ml; –, no plaque formation; +, plaque formation. Schematic representations of invasin and the chimeric cI_N–Inv proteins are shown with the restriction sites used to generate deletions in the chimeric proteins: K, *Kpn*I; RV, *Eco*RV; H, *Hpa*I. The restriction site used for each deletion is indicated by the letter at the deletion endpoints, the internal *Kpn*I and *Hpa*I deletions are in-frame. The cI_N portion of the chimeric proteins is shown as black boxes. The invasin sequences are dark gray boxes, which are aligned in relation to the invasin wild-type sequence shown on the right. The invasion multimerization region is illustrated by dashed lines. Lane 1, JH372/pZ150 (vector); lane 2, JH372/pKH101 ($cI_{N'}$); lane 3, JH372/pJH391 (cI_N–LacZ′); lane 4, JH372/pFG157 (cI wt); lane 5, JH372/pJH370 (cI_N–GCN4); lane 6, JH372/pPD208 (cI_N–Inv478); lane 7, JH372/pPD210 (cI_N–Inv202); lane 8, JH372/pPD213 (cI_N–Inv478Δ*Kpn*I); lane 9, JH372/pPD212 (cI_N–Inv478Δ*Hpa*I); lane 10, JH372/pPD211 (cI_N–Inv478Δ*Eco*RV); lane 11, JH372/pPD223 (cI_N–Inv542–694); lane 12, JH372/pPD226 (cI_N–Inv575–694); lane 13, JH372/pPD228 (cI_N–Inv575–657); and lane14, JH372/pPD244 (cI_N–Inv593–694).

chimera positive control (Figure 5, lane 6). In contrast, the cI_N–Inv202 protein was unable to restore cI repressor activity (48% repression; Figure 5, lane 7), indicating that this chimera behaves like a monomeric protein. Strains expressing chimeric proteins that result in a functional dimeric or multimeric repressor, such as cI and cI–GCN4, confer immunity against the lytic phage λKH54(ΔcI). In contrast, clones expressing monomeric cI proteins are sensitive to the phage (Hu, 1990). Consistent with previous results, bacterial strains expressing cI–Inv478 were immune to the bacteriophage, implying multimer formation, while cI_N–Inv202 failed to allow immunity to the phage (Figure 5).

To characterize further the region of the invasin protein that is responsible for functional cI repressor formation, several deletion derivatives of cI_N–Inv478 were constructed (Figure 5, lanes 8–10). The cI_N–InvΔHpa and cI_N–Inv509–710 proteins, carrying deletions in the invasin C-terminus that destroyed the cell adhesion domain, showed full repressor activity (90 and 94% repression, respectively) and conferred resistance to bacteriophage λKH54, whereas the internal *Kpn*I deletion derivative, cI_N–InvΔKpn, was unable to repress λP_R transcription fully, and bacteria expressing this derivative were sensitive to λKH54 (Figure 5, lanes 8–10). Thus, the region responsible for protein–protein interaction was localized in the internal conserved module II displayed in Figure 1A, consistent with the results from the *in vivo* cross-linking experiments (Figures 3B and 4). Twelve different PCR-derived cI_N–Inv fusions encoding different portions of the invasin module II were analyzed to determine the smallest region capable of stimulating repression by cI. All cI_N–Inv constructs containing amino acids 596–694 of the invasin protein fully repressed λP_R-*lacZ* expression, showing >79% repression, and were resistant to phage KH54 (Figure 5, lanes 11–13). Shorter derivatives failed to show repression (Figure 5, lanes 14 and 15), so this domain may be the minimal region necessary for self-association.

Multivalency stimulates invasin-mediated internalization

Several lines of evidence in this report indicate that a multimeric form of the invasin protein of *Y.pseudotuber-*

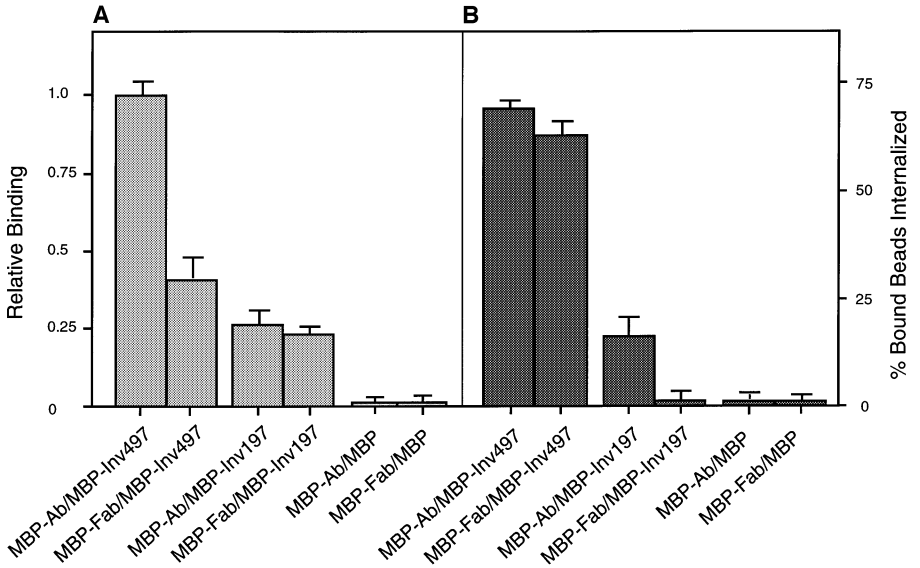

Fig. 6. Increasing ligand valency stimulates invasin-mediated uptake. Binding and uptake efficiency of latex beads coated with size-fractionated MBP–Inv197 or MBP–Inv497 fusion proteins is shown. Latex beads (5×10^6) were coated and used to challenge HEp-2 cells as described (Materials and methods). The total number of cell-associated beads were visualized and determined with phase contrast microscopy while internalized beads were identified by immunofluorescence of non-permeablized cells. The percentage of cell-associated and intracellular beads per cell is shown graphically. Beads coated with different combinations of MBP fusion proteins, antibodies and Fab fragments are illustrated below the graph.

culosis may be the active player in the bacterial uptake process. Therefore, artificially produced bivalent invasin containing the C-terminal cell adhesion region was tested for its ability to promote bacterial uptake relative to a monomeric derivative. The MBP–Inv197 hybrid protein was size-fractionated, and the peak fraction corresponding to the 60 kDa monomer was isolated from aggregated protein found in this preparation (Saltman *et al*., 1996). This fraction was then incubated with latex beads coated with either purified monomeric Fab fragment directed against MBP, or purified anti-MBP, the latter of which should generate bivalent invasin. The coating of the beads was adjusted to allow an identical amount of hybrid protein to be bound for each derivative, and beads adjusted in this fashion were used to challenge HEp-2 cells to assay for internalization, using the fluorescence challenge strategy (see Materials and methods). Beads coated with the monomeric MBP–Inv197 protein bound equally well when coated in either a monovalent or bivalent fashion, yet the entry efficiencies were significantly affected by the valency of coating (Figure 6). Beads coated with monomeric Fab fragment and MBP–Inv197 were not internalized efficiently and uptake was only slightly higher than that observed with MBP, bound to either anti-MBP antibody or Fab fragment (Figure 6). In contrast, up to 20% of the adherent beads coated with monomeric MBP–Inv197 that had been made artificially bivalent by antibody entered HEp-2 cells (Figure 6, MBP–Ab/MBP–Inv197). Therefore, increasing the valency significantly enhanced uptake of this derivative without altering adhesion.

As seen above (Figures 1B–E and 2), beads coated with the Inv497 derivative bound somewhat better than Inv197-coated beads. Surprisingly, beads coated with MBP–Inv497 and divalent antibody had a higher adhesion efficiency than those coated with Fab fragment-linked Inv497. In contrast to the Inv197-coated beads, dimerization of the Inv497 derivative had only a minor stimulatory effect on uptake efficiency of bound beads. Both Fab and antibody-coupled Inv497 proteins resulted in 50–60% entry of all cell-adherent beads (Figure 6), suggesting that the valency of Inv497 alone was sufficient to promote uptake of bound beads.

MBP–Inv497 internalization and integrin redistribution

It has been well established that ligand- and antibody-induced clustering of β_1 integrins can mediate transmembrane signal transduction, inducing a variety of cellular responses (Kornberg *et al*., 1991; Miyamoto *et al*., 1995a). Therefore, binding of invasin to β_1 integrins was studied by analyzing the distribution of MBP–Inv derivatives on cultured cells after short incubation times. Size-fractionated MBP–Inv197 and MBP–Inv497 were added directly to adherent HEp-2 cells, incubated at 20°C for various times and fixed samples were probed by immunofluorescence to visualize protein distribution on the cell surface (Figure 7). In HEp-2 cells exposed to MBP–Inv197, the distribution of the protein was somewhat concentrated on the cell margins, with few patches evident (Figure 7C and G). When cells were incubated with the size-fractionated MBP–Inv497 derivative, however, the protein was observed as focal patches on the cell surface. Occasional redistribution of invasin–integrin complexes was apparent 7 min after addition of MBP–Inv497 to cells (Figure 7D), with significant accumulation of distinct punctate clusters found at 60 min after addition of the protein (Figure 7H). No punctate forms were observed for MBP–Inv197 at this time point (Figure 7G). Patches were also observed on control cells treated with anti-β_1 integrin antibody, although the aggregates were larger and less frequent than that seen for MBP–Inv497 (Figure 7B and F). No such forms were seen on cells exposed to purified MBP (Figure 7A and E).

The patches of invasin appear to be a reflection of the fact that the MBP–Inv497 derivative is internalized,

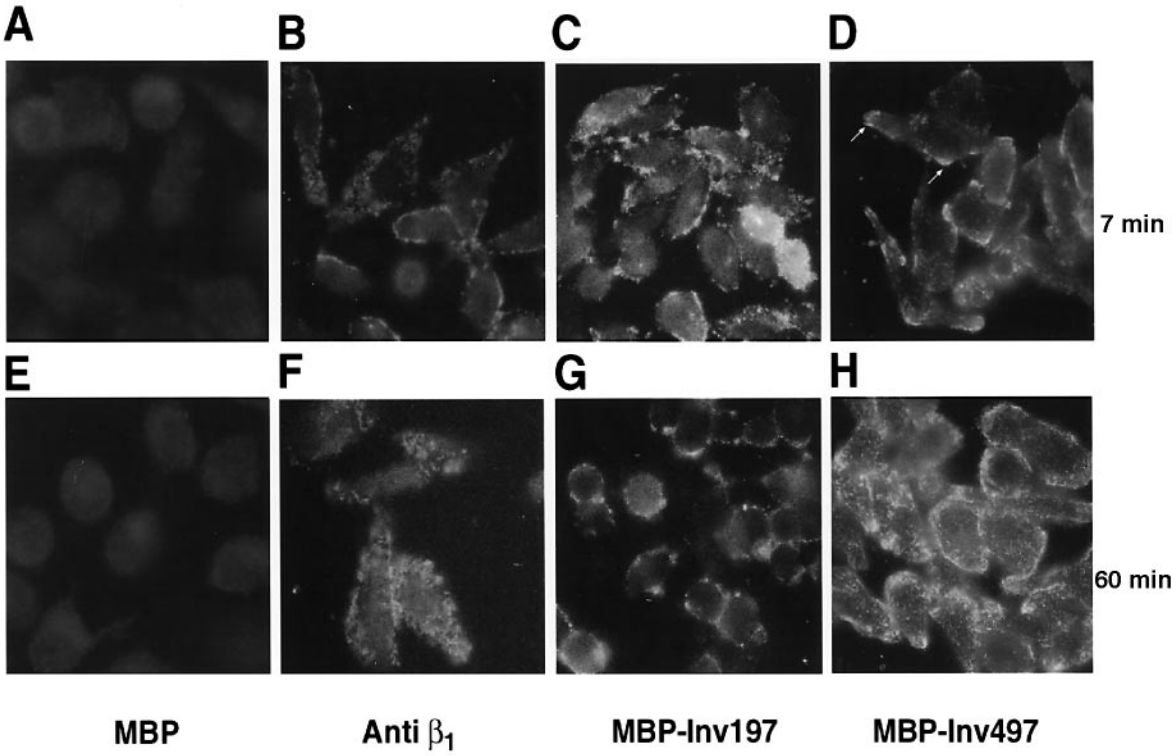

Fig. 7. Invasin-mediated clustering. HEp-2 cells were incubated for 7 (A–D) and 60 min (E and F) with 10 μg/ml purified MBP (**A** and **E**), 5 μg/ml anti-β_1 integrin antibodies VD1 (**B** and **F**), MBP–Inv197 (**C** and **G**) or MBP–Inv497 (**D** and **H**), respectively, in the absence of permeabilization. Cells were fixed with 2% paraformaldehyde and localization of the proteins on the cell surface was visualized by immunfluorescence microscopy using MBP antibodies and FITC-conjugated secondary antibodies. Some local patches of Inv protein at sites of focal adhesions are indicated by arrows.

whereas the the smaller derivative is not. This is based on analysis of the internalization of invasin derivatives and their ability to induce redistribution of integrin receptors. HEp-2 cells incubated with the invasin derivatives MBP–Inv497 or MBP–Inv197 were probed differentially with anti-MBP, either before or after permeabilization, to determine if the cell-associated invasin was internalized (Figure 8). Confocal microscopy revealed that 7 min after binding, both of the derivatives were localized primarily extracellularly, with little intracellular staining by the antibody (Figure 8A and B; external invasin derivatives colored yellow or red). In contrast, by 60 min post-incubation, the MBP–Inv497 derivative was largely internalized (Figure 8D; internal invasin visualized as green), whereas the the MBP–Inv197 was localized mostly at the edges of cells on the external surface (Figure 8C). Cells challenged with invasin derivatives in this fashion, fixed and probed with anti-β_1 integrin antibody, gave results that were consistent with the above analysis. HEp-2 cells incubated with invasin derivatives for short periods of time or extensively with MBP–197 resulted in integrin receptor that was localized largely around the edges of cells, when viewed ~0.6 μm above the adhesion plane (Figure 8E–G). In contrast, 60 min of incubation of HEp-2 cells with the MBP–Inv497 derivative caused significant redistribution of the integrin receptor (Figure 8H). These results indicate that after binding to HEp-2 cells, clustering and internalization of invasin, as well as redistribution of integrin receptor, were all enhanced for Inv497 relative to Inv197.

Discussion

In previous studies, it has been shown that the C-terminus of invasin is essential for binding and uptake, and can promote entry when coated on non-adherent bacteria (Leong *et al*., 1990; Rankin *et al*., 1992). It has been assumed that bacterial uptake promoted by invasin is strictly a result of the ability of the protein to adhere to integrins. In this study, we report the identification and analysis of an additional property of invasin necessary for high efficiency uptake. Moreover, evidence is presented that a specific domain linked to this activity has the capacity to mediate intermolecular interaction. Using a bead challenge assay, we showed that particles coated with low concentrations of a purified fragment comprising the C-terminal cell-binding domain of invasin (Inv197) adhered to epithelial cells, but showed little internalization. In contrast, beads coated with a larger invasin derivative comprising the C-terminal 497 amino acids of invasin (Inv497) were internalized far more efficiently even at low coating concentrations (Figure 2). Protein sequences present in Inv497, but absent in Inv197, appeared to enhance entry and contributed to the high efficiency of invasin-mediated uptake.

The region of invasin necessary to promote enhanced uptake contains a specific domain that is capable of promoting intermolecular interaction and is located within a region of the protein required for chemical cross-linking on the bacterial cell surface. We examined various invasin derivatives by chemical cross-linking and found that the invasin wild-type protein, as well as the deletion product

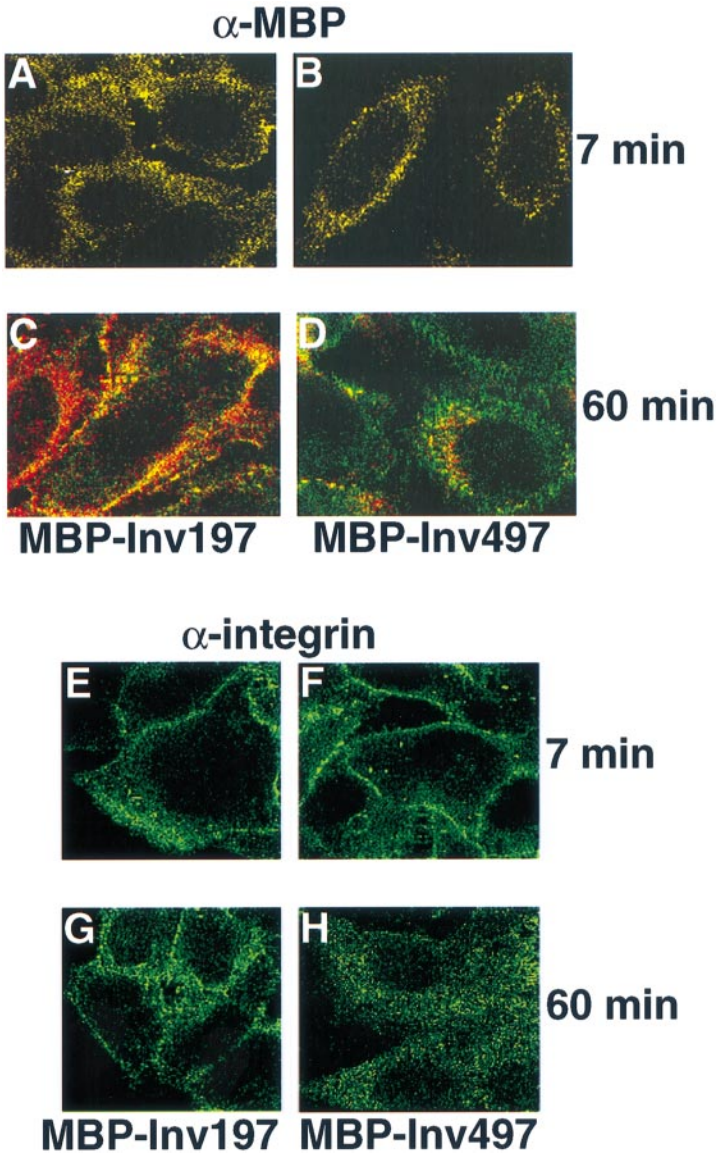

Fig. 8. Inv497 derivative is internalized by HEp-2cells. HEp-2 cells were incubated for 7 min (A, B, E and F) or 60 min (C, D, G and H) with 10 μg/ml of purified size-fractionated MBP–Inv derivatives. (**A**–**D**) After fixation, cells were probed with anti-MBP and Texas Red-conjugated secondary antibody to visualize surface-exposed invasin derivatives. After 20 s permeabilization by methanol at –20°C, the cells were probed once again with anti-MBP and FITC-conjugated secondary antibody to visualize both external and internalized protein. Samples were analyzed by confocal microscopy, and sections ~2.4 μm above the extracellular matrix are shown. Only protein that has been internalized will resist staining by the IgG–Texas Red, and will be visualized as green. Protein that remains surface localized will either stain red (saturating staining by IgG–Texas Red prior to permeabilization) or yellow (staining both prior to and after permeabilization by IgG conjugates). HEp-2 cells incubated with MBP–Inv197 (A and C) or MBP–Inv 497 (B and D) prior to fixation. (**E**–**H**) After fixation, separate samples of cells were probed with rabbit polyclonal anti-β_1 integrin and FITC-conjugated secondary antibody to visualize integrin localization. Samples were visualized by confocal microscopy, and sections ~1.2 μm above the extracellular matrix are shown. HEp-2 cells incubated with MBP–Inv 197 (E and G) or MBP–Inv 497 (F and H) prior to fixation. Note that only after incubation with MBP–Inv497 for 60 min is there significant redistribution of integrin receptor away from the edges of the cells.

InvΔHpa and the purified Inv497 derivative, formed species with apparent molecular weights consistent with multimerization. In contrast, no oligomeric complexes were found with the deletion product InvΔKpn and the Inv197 protein (Figures 3B and 4), indicating that the sequences responsible for protein–protein interaction are absent from these derivatives. The identification of dominant-interfering mutations located in the C-terminal integrin recognition site of the protein is also consistent with the property of multimerization.

Invasin sequences encompassing amino acids 596–694 of the invasin protein fused to the monomeric DNA-binding domain of cI caused stimulation of repressor function (Figure 5). This region is located N-terminal to the extracellular cell adhesion domain that recognizes integrin receptors (Figure 1A) and previously had not been assigned a specific function. Preliminary crystallographic analysis (Z.A.Hamburger and P.J.Bjorkman, unpublished data) of the Inv497 peptide indicate that the smallest region competent to confer high-level repression demarks the endpoints of a distinct globular domain. This region stands out by having a large number of uncharged amino acids (76 out of 99 amino acids; Figure 9A).

The most striking result is the demonstration that bivalent invasin complexes are more powerful mediators of uptake than their monovalent counterparts (Figure 6).

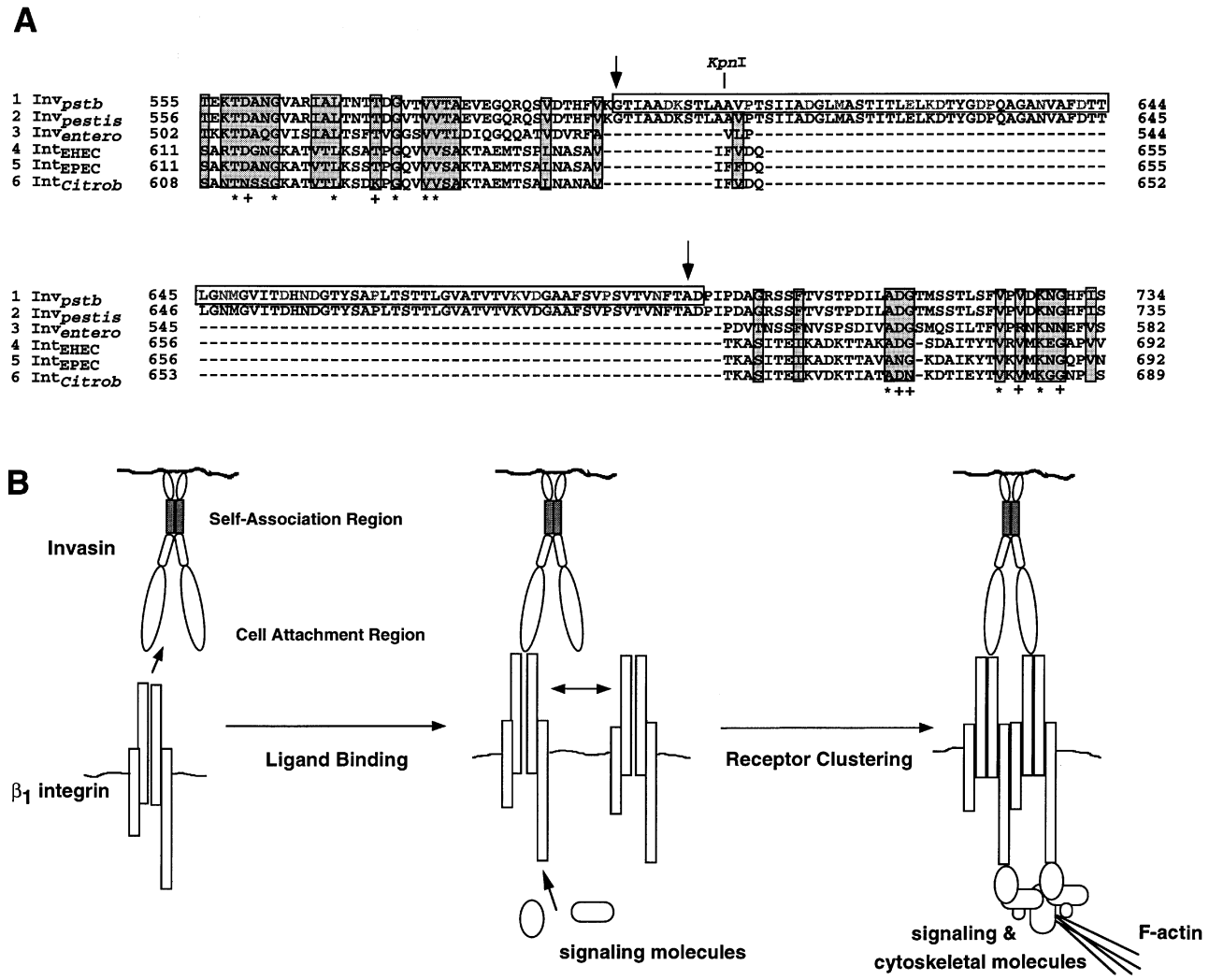

Fig. 9. (**A**) Amino acid sequence alignment of module II of invasin and intimins. The predicted amino acid sequence (amino acids 555–734) of invasin from *Y.pseudotuberculosis* is shown (Isberg *et al*., 1987), aligned with the sequences of invasin of *Y.pestis* (Simonet *et al*., 1996) and *Y.enterocolitica* (Young *et al*., 1990), and sequences of intimins of enteropathogenic *E.coli* (EPEC) (Jerse *et al*., 1990), enterohemorrhagic *E.coli* (EHEC) and *Citrobacter freundii* strains (Schauer and Falkow, 1993; Frankel *et al*., 1994). Sequences were aligned using the program Clustal W (Altschul *et al.*, 1990). Residue numbers of each protein are given at the start and the end of each line. Identical amino acid residues found among all five are noted as asteriks (*), whereas (+) denotes a match of four out of five proteins. Similar amino acid residues found in at least four of the five proteins are enclosed by thin, shaded boxes.The boxed sequence of the *Y.pseudotuberculosis* invasin represents the domain responsible for full cI_N-mediated repression/invasin multimerization. The dashes indicate the region that is deleted in the *Y.enterocolitica* Inv and in intimins. (**B**) Clustering model of invasin-mediated uptake into mammalian cells. Multivalent invasin induces integrin clustering through simultaneous binding to more than one integrin heterodimer. Depending on ligand binding and the multimerization state of the β_1-integrin, different cell signaling molecules associate and trigger the association of other signaling and cytoskeletal proteins.

We showed that size-fractionated monomeric invasin derivative Inv197 immobilized on latex beads by divalent antibodies promoted far more internalization than when it was immobilized by monomeric Fab fragments. Interestingly, the invasin protein of *Y.enterocolitica*, which permits 6- to 60-fold less efficient uptake by cultured cells than the *Y.pseudotuberculosis* protein (Pepe and Miller, 1990), is missing the domain required for protein–protein interaction (Figure 9A). As expected from this study (Figure 2), high production levels of the *Y.enterocolitica* protein can compensate for the absence of this domain (data not shown). The intimins encoded by enteropathogenic *E.coli* strains (EHEC, EPEC) and *Citrobacter freundii*, which are homologous to invasin, also apparently lack this particular region (Figure 9A). Intimins are involved normally in the formation of special attachment and effacing structures (pedestals) on the host cell surface, which immobilize the bacteria extracellularly without causing large-scale bacterial uptake (Jerse *et al*., 1990; Frankel *et al*., 1994). The behavior of the *Y.enterocolitica* invasin is similar to that of an invasin deletion derivative (InvΔKpn) that has most of the enhancer region removed. This derivative could not be cross-linked (Figure 4) and promoted entry at only 4% the efficiency of the wild-type protein (Table II). Thus, lack of multivalency strongly correlates with a lower uptake efficiency, emphasizing the importance of invasin–invasin interaction for the internalization process.

The simplest explanation for why uptake is enhanced by multimerization is that clustering results in increased affinity of invasin for its integrin receptors (Tran Van Nhieu and Isberg, 1993a). Previous studies have shown that two

Table III. Bacterial strains, plasmids and bacteriophages

Strains/plasmid/phage	Description	Origin/reference
E.coli K12		
SR2	F⁻ *araD* Δ*(lacU)* Δ*phoA lpp5508 galE rpsL galE galK degP::*Tn*5*	Rankin *et al*. (1992)
XAcSu6	F⁻ *araD D(lac-pro)X111 argE$_{am}$ rifR nalR met*⁻	John Leong
XAcSu6(λgt11*inv* Δ8–15)	pRI221/Δ8–15(*inv*$^+$) crossed into XAcSu6	John Leong
XLIblue	F′::Tn*10 proA*$^+$*B*$^+$ *lacI*^{q} Δ(*lacZ*)M15/*recA1 endA1 gyr*A96 (Nal^r) *thi hsdR17* ($r_K^-m_K^+$) *supE44 relA1 lac*	laboratory stock
JH372	lysogenic λ202 (*imm* 21 P_R-*lacZ*ΔO_R2)	Hu (1990)
Y.pseudotuberculosis		
YPIII(P⁻)	*inv*$^+$, cured of pIB1	Bolin *et al*. (1982)
Plasmids		
pFG157	λcI *ind1*, *lacUV5* promoter, colE1 *ori*, Amp^R	Hu (1990)
pJH370	λcI *ind1* amino acids 1–132 fused to zipper domain of GCN4	Hu (1990)
pJH391	λcI *ind1* amino acids 1–132 fused to *lacZ′*, Amp^R	Hu (1990)
pJL206	produces Inv*ΔHpa*I in-frame deletion, Amp^R	Isberg and Leong (1988)
pJL272	produces wild-type invasin (*inv*$^+$), Amp^R	Leong *et al*. (1993)
pJL272-D911E	produces InvD911T (Asp→Glu), Amp^R	Leong *et al*. (1993)
pJL316-D911T	produces InvD911T (Asp→Thr), Amp^R	Leong *et al*. (1995)
pKH101	λcI *ind1* amino acids 1–132[a], Amp^R	Hu (1990)
pPD208	produces cI_N–Inv509–986[a](Inv478), Amp^R	this work
pPD210	produces cI_N–Inv795–986[a](Inv202),Amp^R	this work
pPD211	produces cI_N–Inv509–710[a](Δ*Eco*RV), Amp^R	this work
pPD212	produces cI_N–Inv509–607/795–986[a](Δ*Kpn*I), Amp^R	this work
pPD213	produces cI_N–Inv509–803/851–986[a](Δ*Hpa*I), Amp^R	this work
pPD214	produces Inv*ΔHpa*I in-frame deletion, Amp^R	this work
pPD223	produces cI_N–Inv542–694[a], Amp^R	this work
pPD224	produces cI_N–Inv542–657[a], Amp^R	this work
pPD226	produces cI_N–Inv575–694[a], Amp^R	this work
pPD228	produces cI_N–Inv575–657[a], Amp^R	this work
pPD244	produces cI_N–Inv596–694[a], Amp^R	this work
pRI203	pBR325 *inv*$^+$, Amp^R	Isberg *et al*. (1987)
pRI207	produces Inv*ΔKpn*I in-frame deletion, Amp^R	laboratory stock
pRI284	produces MBP–Inv197 fusion protein	this work
pRI285	produces MBP–Inv497 fusion protein	Leong *et al*. (1995)
pSelect-2	cloning plasmid for *in vitro* mutagenesis, Tet^R	Promega
pSelect-2-8	pSelect-2 (*inv*$^+$), produces wild-type Inv, Tet^R, Amp^R	Saltman *et al*. (1996)
pSelect-2-8-D911A	pSelect-2, produces InvD911A, Tet^R, Amp^R	Saltman *et al*. (1996)
pZ150	cloning vector carrying *lacUV5* promoter, Amp^R	Hu (1990)
Bacteriophages		
λKH54	Δ*c*I	Hu (1990)

[a]Protein expressed from the lacUV5 promoter.

critical determinants that modulate invasin-mediated uptake are integrin receptor density and the relative affinity at which the ligand binds receptor (Tran Van Nhieu and Isberg, 1993a; Leong, *et al*., 1995). Efficient uptake requires high affinity binding to the integrin receptor, while low affinity ligands promote bacterial adhesion to the mammalian cell without subsequent uptake (Tran Van Nhieu and Isberg, 1993a). Monomeric invasin may be of insufficient affinity to promote efficient uptake of *Y.pseudotuberculosis*, and multimerization would increase the binding affinity sufficiently to promote efficient uptake. A precedent for this phenomenon has been noted with the intracellular adhesion molecule-1 (ICAM-1), a potent β_2 integrin ligand on lymphocytes. This protein forms homodimers at the host cell surface which enhance its activity in cell adhesion relative to its monomeric derivatives of ICAM-1 (Miller *et al*., 1995).

An alternate model proposes that multimerization is required to send a necessary signal. Invasin multimers, containing multiple receptor-binding domains, might interact simultaneously or cooperatively with several receptor molecules, inducing conformational changes and/or receptor clustering (Figure 9B). Results obtained in recent years provide evidence that multivalent ligand-induced receptor oligomerization and clustering are required to trigger a large number of intracellular signaling events generated by integrin receptors (Kornberg *et al*., 1991; Miyamoto *et al*., 1995a,b). The elucidation of signal transduction pathways involved in integrin-mediated signaling has revealed that the activity of tyrosine kinases and other signaling molecules as well as the participation of cytoskeletal components in these pathways is regulated by the nature of the bound ligand and the multimeric state of the integrin receptor (Miyamoto *et al*., 1995a,b). Similarly, oligomerization by multivalent invasin binding may generate the crucial signal to recruit appropriate signaling molecules and cytoskeletal elements for bacterial uptake (Figure 9B). By the clustering model, close proximity of receptors in a relatively small area of the cell surface would be essential for signal transmission. As receptor clustering is predicted to be sufficient to transmit an internalization signal, a high concentration of a monomer should promote entry as efficiently as a lower concentration of multimeric ligands (Figures 1 and 6).

The results of sedimentation analysis of the soluble C-terminus of invasin (Table I), the low efficiency of cross-linking (Figure 4) and crystallographic analysis of the C-terminal 497 amino acids (Z.A.Hamburger and

P.J.Bjorkman, unpublished data) indicate that invasin may exist primarily as a monomer in the absence of membrane localization. By limiting diffusion of the protein to two dimensions, the outer membrane may stabilize transient multimer formation, particularly for individual processing products of invasin. In fact, preferential multimerization can be observed for a 70 kDa C-terminal invasin fragment, which was cross-linked quantitively (Figure 4), indicating that it may exist entirely in a multimeric form. Further studies on the oligomerization state of invasin in the presence and absence of receptor binding should reveal if multimerized species are bound more efficiently to the integrin receptor.

Enteropathogenic *Yersinia* have developed a special strategy to usurp normal cellular functions (Tran Van Nhieu *et al*., 1996). Similar strategies have been seen in a large number of pathogens (Finlay and Cossart, 1997). In the present work, we have identified a novel role for multivalent ligand interaction in uptake and proposed invasin-induced receptor oligomerization as a crucial step in efficient bacterial uptake. Future work should provide more information about the specific nature of the association between invasin and its receptor and allow deeper insight into integrin-mediated signal transduction pathways.

Materials and methods

Bacterial strains, cell culture and media

Bacterial strains used in this study are listed in Table III. Overnight cultures of *E.coli* were grown at 37°C, *Yersinia* strains were grown at 28°C in Luria–Bertani medium. HEp-2 cells were cultured in RPMI 1640 media (Irvine Scientific) supplemented with 5% newborn calf serum (Life Technology Inc.) and 2 mM glutamine at 37°C in the presence of 5% CO_2.

DNA manipulations, plasmids and oligonucleotides

Preparations of plasmid DNA and phages, restriction digestions, ligations and transformations were performed as previously described (Sambrook *et al*., 1989; Miller, 1992). PCR reactions were performed in a standard 100 µl mix for 20 cycles in a DNA thermal cycler PTC-200 (MJ Research). PCR products were purified with the QIAquick Kit (Qiagen) before and after restriction digestion of the amplification products.

Plasmids used in this study are listed in Table III. Plasmids pRI284 and pRI285 were constructed by fusing a PCR-derived fragment of the *inv* gene of *Y.pseudotuberculosis* encoding the C-terminal 197 and 497 amino acids of invasin to the *malE* gene of pMal-c1 (New England Biolabs) inserted in the *Xba*I and *Hin*dIII sites. Plasmids pPD208 (*cI_N–inv478*) and pPD210 (*cI–inv202*) were constructed by fusing a PCR-derived fragment containing codons 509–986 and 795–986 of the *Y.pseudotuberculosis inv* gene in-frame with cI_N at the *Sal*I site on vector pJH391 (Hu, 1990). The following primers were used. Forward primer *inv478*, 5′-TAACGTCGACCGTCATTGGTGATGGC-3′; forward primer *inv202*, 5′-CCCTGTCGACGGTACCTACGCTGACC-3′; reverse primer *inv478* and *inv202*, 5′-CCAGGATCCTGGGCCGTAAGATCGG-3′. The *inv* in-frame deletions of plasmids pPD211, pPD212 and pPD213 were derived from plasmid pPD208 by *Eco*RV (*cI–inv509–710*), *Kpn*I (*cI–inv509–608,795–986*) or *Hpa*I (*cI–inv509–803,851–986*) digests and religations. The plasmids pPD223, pPD226–227 and pPD244 were constructed by inserting PCR-derived *Sal*I–*Bam*HI fragments containing codons 542–694 (pPD223), 575–694 (pPD226), 575–657(pPD227) and 593–694 (pPD244) using the upstream primers 5′-GGGGGGTCGACGGTGATAACCACCAATAATGGTGCG-3′, 5′-GGGGGGTCGACCGTGACGGTAGTCACAGCAGAAGTGG-3′ and 5′-GGGGGGTCGACAAGGGTACTATCGCGGCGGATAAATCC-3′, and the respective downstream primers 5′-CCGCGGGATCCCTTAATCTGCCGTGAAATTAACCG-3′ and 5′-CCGCGGGATCCCTTAGCCGTCATTGTGATCCGTGATAAC-3′. Oligonucleotides were synthesized by the Howard Hughes Medical Institute Microchemical Facility, Harvard Medical School.

β-Galactosidase assay

Escherichia coli strains JH372 harboring derivatives of pJH391 were grown overnight at 37°C. To lyse the cells, 20 µl of 0.1% SDS and 40 µl of chloroform were added to 100 µl of the culture and incubated for 5 min at room temperature. Assay of β-galactosidase was performed as described by Miller (1992) and activity was calculated as follows: β-galactosidase activity = $[OD_{420}$ assay$]\times 6.75/[OD_{600}$ cells$]\times$min (time of reaction)$\times$0.1 ml (reaction volume).

In vitro and in vivo cross-linking

For *in vitro* cross-linking, various concentrations of formaldehyde (37% w/w, Fisher) or Sulfo-EGS (Pierce, USA) were added to 10 µg of purified Inv497 protein in 25 mM HEPES (pH 7.0), 1 mM EDTA. Samples were incubated for 30 min at room temperature with gentle shaking rotation, and reactions were stopped by adding ethanolamine (pH 7.4) in a final concentration of 50 mM. Prior to 10% SDS–PAGE, a portion of a sample containing no or 0.8% formaldehyde was heated for 15 min at 100°C, to reverse the cross-linking. Samples were analyzed by 10% SDS–PAGE, followed by immunoblotting using anti-invasin mAb3A2 (Leong *et al*., 1990). For *in vivo* cross-linking, XL1blue harboring invasin derivatives was grown in L broth with 100 µg/ml ampicillin at 37°C to an OD_{600} = 0.7. The cells were harvested by centrifugation, washed once, either with $NaPO_4$ buffer (pH 7.5) for formaldehyde or 10 mM HEPES (pH 7.5), 1 mM EDTA for BS^3 (Pierce) and Sulfo-EGS (Pierce) cross-linking, and resuspended in the identical buffers to an OD_{600} = 1.0. The reactions were allowed to proceed at 0°C for 1 h with shaking and were terminated in the presence of ethanolamine, as above. Samples were washed twice with the reaction buffer containing ethanolamine. Pellets were resuspended in 40 µl of sample buffer and aliquots of 10 µl were analyzed by 10% SDS–PAGE followed by immunoblotting using invasin antibodies mAb3A2 and mAb2A9 (Leong *et al*., 1990).

Covalent coupling of protein and antibodies to latex beads

About 10^8 latex beads (1.1 µm diameter, Sigma) were placed in glass centrifuge tubes and washed sucessively in 1 ml of phosphate-buffered saline (PBS) and 1 ml of 0.2 M Na_2HCO_3 (pH 8.5), 0.5 M NaCl (coupling buffer) and were resuspended in 100 µl of coupling buffer. Purified Inv197 and Inv497 proteins (isolated as described earlier) were added in a range of concentrations from 0 to 1 mg/ml. Proteins were allowed to adsorb to the beads for 30 min at 37°C. Subsequently, 20 µl of biotinylated BSA (1 mg/ml) was added and incubated for an additional 30 min at 37°C. After adding 500 µl of coupling buffer to the beads, the solution was sonicated for 20 s, and 500 µl of 20 mg/ml BSA in coupling buffer was added and incubated at 37°C for an additional hour to complete blocking. The beads were washed in PBS containing 10 mg/ml BSA and stored in 200 µl of PBS containing 2 mg/ml BSA at 4°C. The coupling efficiency, and protein concentrations of the starting solution added to beads and the supernatant before addition of BSA were determined using the BCA Kit (Pierce). For anti-MBP Ab/Fab-coated beads, the beads were prepared in a similar manner and coated at 200 µg/ml. To allow coupling of the invasin derivatives, the Ig-coated beads were incubated with 50 µg/ml of size-fractionated MBP–Inv197 and MBP–Inv497 protein in PBS containing 1% BSA at 4°C overnight, washed three times with PBS to remove unbound protein and stored in PBS with 0.2% BSA.

To determine the number of invasin molecules on beads, purified proteins were labeled with carboxytetramethyl rhodamine, succinimidyl ester (Molecular Probes, Inc.) as described (Rankin *et al*., 1992) or analyzed by surface enzyme-linked immunosorbent assays (ELISAs), as follows: 1:2 dilutions of 10^8 beads were washed in PBS and incubated with primary anti-invasin antibody mAb3A2 at room temperature in PBS containing 2% goat serum for 1 h. Subsequently, beads were washed three times with PBS and incubated with anti-mouse IgG–alkaline phosphatase at room temperature for an additional hour. After three subsequent washes alkaline phosphatase assays were performed with 1 mg/ml σ^{104} (Sigma) in AP-buffer (100 mM Tris–HCl pH 9.5, 5 mM $MgCl_2$, 150 mM $NaCl_2$) and quantitated at 405 nm with a microtiter spectrophotometer (BioRad). The amount of invasin on the bead was then quantitated and calculated from standard ELISAs of the same protein coated on plastic. To this end, serial dilutions of the protein were incubated on 96-well plates for 16 h at 4°C, and the amount of bound protein was determined by subtraction of the amount of remaining protein in the supernatant from that of the in-put protein.

Internalization of bacteria into mammalian cells, quantitation of cell binding of invasin-expressing bacteria and quantitation of invasin proteins on the surface of bacteria

Penetration of bacteria into cultured mammalian cells was assayed by gentamicin protection assays, as described (Leong *et al*., 1990).

Approximately 5×10^5 *E.coli* bacteria expressing the wild-type *inv* gene or various *inv* mutations were centrifuged onto a subconfluent HEp-2 cell monolayer and incubated for 90 min at 37°C. Extracellular bacteria were then killed by a 90 min treatment in the identical media containing 50 μg/ml gentamicin. The surviving intracellular bacteria were released with 0.1% Triton X-100, and viable counts were titered on bacteriological media. For each individual clone, the relative level of bacterial uptake was determined by calculating the number of colony-forming units that arose relative to the total number of bacteria in the assay.

Surface expression of invasin proteins was determined by mAb3A2 and mAb2A9 probing. Bacteria were incubated in PBS containing 2% goat serum and 1 μg/ml primary anti-invasin antibodies mAb3A2 or mAb2A9 followed by reprobing with 5 μg/ml goat anti-mouse IgG alkaline phosphatase (Zymed) for 1 h at room temperature. The cell density was determined at A_{600}, and the bacteria were incubated in AP-buffer with 1 mg/ml σ^{104} alkaline phosphate substrate to assay for bound antibody, as described earlier.

Cell binding of bacteria expressing invasin derivatives was determined as described (Leong *et al*., 1995).

Expression and purification of invasin proteins

Twenty liters of SR2 (pRI284) or SR2 (pRI285) were grown at 28°C in L broth to an $A_{600} = 0.6$. Isopropyl-β-D-thiogalactopyranoside (IPTG) was added to final concentration of 1 mM to induce the expression of MBP–Inv fusions. The cells were grown for an additional 2 h before being harvested. Frozen cell pellets were resuspended in 50 ml of 10 mM Tris pH 8.0 plus protease inhibitor cocktail containing 5 mM phenylmethylsulfonyl fluoride (PMSF), 10 mM pepstatin (Sigma), 10 mM E64 protease inhibitor (Boehringer Mannheim, Germany), 20 μM leupeptin (US Biochemical) and 10 μM chymostatin (Sigma). The MBP–Inv197 protein was purified by affinity chromatography on cross-linked amylose, as described previously (Leong *et al*., 1990; Rankin *et al*., 1994). MBP–Inv497 was purified by ion exchange chromatography, with slight modification of previous procedures (Leong *et al*., 1995). A cell extract containing MBP–Inv497 was loaded onto a HiLoad 26/10, Fast Flow Q Sepharose column (Pharmacia, Biotech, Inc.) equilibrated with 10 mM Tris pH 8.0 and eluted with a continous salt gradient (0–500 mM NaCl). The MBP–Inv497 protein that eluted at ~100–120 mM NaCl was pooled, precipitated in 40% ammonium sulfate, resuspended in 10 mM Tris pH 8.0 plus protease inhibitor cocktail and dialyzed twice against 100 volumes of the same buffer. Subsequently, the protein was reloaded on the Q Sepharose column and pure peak fractions were pooled. To liberate Inv 497 and Inv197 proteins from the MBP moiety, both proteins were cleaved by factor Xa (New England Biolabs) adding 0.5 mg of protease per 100 mg of fusion protein in factor Xa cleavage buffer (15 mM Tris pH 8.0, 100 mM NaCl, 2 mM $CaCl_2$), and incubated at 14°C for 12 h. The protease reaction was stopped by 10 μM 1,5-DNS-GGACK-HCl inhibitor (Calbiochem) and the MBP protein was removed by loading the samples on a cross-linked amylose column equilibrated with 15 mM Tris–HCl (pH 8.0). Pure Inv497 and Inv197 were collected from the column flowthrough, and protein concentrations were determined by the BCA protein assay (Pierce).

Gel filtration

A portion of the MBP–Inv proteins aggregate into soluble higher molecular weight complexes. To isolate MBP–Inv197 and MBP–Inv497 hybrid proteins from larger complexes, protein preparations were subjected to gel filtration chromatography on a 10 mm×30 cm Superose 12 column (Pharmacia Biotech, Inc.). The column was equilibrated with 20 mM HEPES (pH 7.0) and calibrated using a variety of protein standards with known molecular sizes: 669 kDa thyroglobin, 440 kDa ferritin, 232 kDa catalase, 158 kDa aldolase, 67 kDa BSA and 43 kDa ovalbumin. Samples (200 μl) of the MBP–Inv fusion proteins (5 mg/ml) were applied to this column and collected in 200 μl fractions. Proteins eluted in the void volume were discarded and peak fractions corresponding to the MBP–Inv197 and the MBP–Inv497 species in the included volume were pooled and concentrated using a Centricon 30 filter (Amicon, Beverly, MA). Thereafter, samples were refractionated on an identical gel filtration column to ensure that no aggregation of the purified sample occurred on storage and concentration.

Analytical gel filtration of purified Inv197 and Inv497 cleaved from MBP was identical to above, using 1 mg/ml Inv197 and 4 mg/ml Inv497, respectively. Elution profiles were monitored by UV absorption, and 200 μl fractions were collected and probed by immunoblotting using anti-invasin mAb 3A2.

Purification of anti-MBP and anti-MBP–Fab fragments

A 500 μl aliquot of anti-MBP serum was diluted with 1 ml of 10 mM Tris–HCl (pH 7.5) and incubated overnight at 4°C in a roller with 5 ml of a 50% protein A–Sepharose slurry (Pharmacia Biotech, Inc.) equilibrated in the same buffer. The material was poured into a 1×5 cm column (BioRad) and washed with 20 ml of 10 mM Tris–HCl (pH 7.5) and 20 ml of 100 mM Tris–HCl (pH 7.5). Antibodies were eluted with 100 mM citric acid (pH 3.5). The pH of the eluted antibodies was readjusted to pH 7.5 with 1 M Tris–HCl (pH 8.0). To isolate Fab fragments, the purified anti-MBP IgG was incubated in 100 mM sodium acetate (pH 5.5), 50 mM cysteine, 1 mM EDTA containing 10 μg/ml papain/mg of IgG at 37°C overnight. The Fab fragments subsequently were separated from uncleaved Fab and Fc as described (Harlow and Lane, 1988).

Immunofluorescence microscopy

Approximately 5×10^4 HEp-2 cells were seeded and grown on coverslips placed inside individual wells of 24-well cell culture plates (Costar). Cell monolayers were washed three times with PBS and incubated in RPMI 1640 medium supplemented with 20 mM HEPES (pH 7.0) and 0.4% BSA (binding buffer), before the addition of ~5×10^6 beads (corresponding to 100 beads per cell). Beads were centrifuged onto the cell monolayer (1000 r.p.m., 5 min) and incubated at 37°C in a humidified atmosphere of 5% CO_2. At 1 h post-infection, the cells were washed three times with PBS and fixed with 2% paraformaldehyde in PBS for 20 min at room temperature. For differential staining of adherent and internalized invasin-coated latex beads, fixed cell monolayers were incubated sequentially in PBS containing 2% goat serum for 10 min, PBS containing 2% goat serum and 1 μg/ml anti-invasin mAb3A2 for 1 h at room temperature, and PBS containing 2% goat serum and 5 μg/ml anti-mouse IgG–fluorescein isothiocyanate (FITC) for 1 h at 37°C. To detect beads blocked with biotinylated BSA, 5 μg/ml FITC–streptavidin (Pierce) was used. For anti-MBP- or anti-MBP Fab fragment-coated beads, 1 μg/ml rabbit anti-MBP (New England Biolabs) and 5 μg/ml anti-rabbit IgG–FITC (Zymed) was used. Three washes in PBS were performed at the beginning and end of each incubation step. Stained samples were mounted in PBS containing 0.1% *p*-phenylenediamine, 80% glycerol (v/v). Quantification of adherent and internalized latex beads was performed using a Zeiss Axioskope (Jena, Germany) with a fluorescence filter set. The total number of adherent and internalized beads was determined under phase contrast for 200 individual cells, and the number of adherent and intracellular beads per cell was determined as the mean of 50 individual cells. Error bars represent the standard deviations of mean values from four groups of 50 cells counted in various regions of the stained specimens. Data presented correspond to one of three typical independent experiments.

For clustering experiments, HEp-2 cells were seeded and grown on coverslips placed inside individual wells of 24-well cell culture plates (Costar). Cell monolayers were washed three times with PBS and incubated in binding buffer (see above) for 10 min at room temperature, before the addition of 10 μg/ml MBP–Inv197, 10 μg/ml MBP–Inv497 or 5 μg/ml anti-β_1 invasin mAb VD1 (Tran van Nhieu and Isberg, 1993a). The cells were incubated for 7 or 60 min at room temperature and washed three times with PBS to remove unbound protein or antibody. Subsequently, the cells were fixed with 2% paraformaldehyde and incubated successively with anti-MBP (NE Biolabs) and goat anti-rabbit Ig-FITC (Zymed) or goat anti-mouse Ig-FITC (Boehringer Mannheim) in PBS containing 2% goat serum. Three washes in PBS were performed at the beginning and end of each incubation step. Stained samples were mounted in PBS containing 0.1% *p*-phenylenediamine, 80% glycerol (v/v), and clusters visualized by microscopy, as described above.

Acknowledgements

We would like to thank Dr James Hu for providing strains and phages for the one-hybrid assay system, Drs John Leong and Eric Krukonis for providing strains, and Dr Carol Kumamoto for anti-MBP antiserum. We thank Zsuzsa A.Hamburger and Dr Pamela J.Bjorkman for unpublished information, and Dr Pak Poon for running the sedimentation analysis. We also thank Drs Dorothy Fallows, Martin Fenner and Joseph Vogel for helpful discussion and critical reading of the manuscript. This work has been supported by the Howard Hughes Medical Institute and the NIH-Grant RO1-AI23538. P.D. is a recipient of a research fellowship of the Deutsche Forschungsgemeinschaft.

References

Altschul,S.F., Gish,W., Miller,W., Myers,E.W. and Lipman,D.J. (1990) Basic local alignment search tool. *J. Mol. Biol.*, **215**, 403–410.

Bolin,I., Norlander,I. and Wolf-Watz,H. (1982) Temperature-inducible outer membrane protein of *Yersinia pseudotuberculosis* and *Yersinia enterocolitica* is associated with the virulence plasmid. *Infect. Immun.*, **37**, 506–512.

Braun,L., Ohayon,H. and Cossart,P. (1998) The InlB of *Listeria monocytogenes* is sufficient to promote entry into mammalian cells. *Mol. Microbiol.*, **27**, 1077–1087.

Clark,E.A. and Brugge,J.S. (1995) Integrins and signal transduction pathways: the road taken. *Science*, **268**, 233–239.

Devenish,J.A. and Schiemann,D.A. (1981) HeLa cell infection by *Yersinia enterocolitica*: evidence for lack of intracellular multiplication and development of a new procedure for quantitative expression of infectivity. *Infect. Immun.*, **32**, 48–55.

Finlay,B.B. and Cossart,P. (1997) Exploitation of mammalian host cell functions by bacterial pathogens. *Science*, **276**, 718–725.

Frankel,G., Candy,D.C.A., Everest,P. and Dougan,G. (1994) Characterization of the C-terminal domains of intimin-like proteins of enteropathogenic and enterohemorrhagic *Escherichia coli*, *Citrobacter freundii* and *Hafnia alvei*. *Infect. Immun.*, **62**, 1835–1842.

Gruetzkau,A., Hanski,C., Hahn,H. and Riecken,E.O. (1990) Involvement of M cells in the bacterial invasion of Peyer's patches: a common mechanism shared by *Yersinia enterocolitica* and other enterovasive bacteria. *Gut*, **31**, 1011–1015.

Harlow,E. and Lane,D. (1988) *Antibodies: A Laboratory Manual*. Cold Spring Harbor Laboratory Press, Cold Spring Harbor, NY.

Hook,M., Switalski,L., Wastrom,T. and Lindberg,M. (1989) Interactions of pathogenic microorganisms with fibronectin. In Mosher,D.F. (ed.), *Fibronectin*. Academic Press, San Diego, CA, pp. 295–308.

Hu,J. (1990) Sequence requirements for coiled-coils: analysis with lambda repressor–GCN4 leucine zipper fusions. *Science*, **250**, 1428–1431.

Hynes,R.O. (1992) Integrins: versatility, modulation and signaling in cell adhesion. *Cell*, **69**, 11–25.

Isberg,R.R. (1989) Mammalian cell adhesion functions and cellular penetration of enteropathogenic *Yersinia* species. *Mol. Microbiol.*, **3**, 1449–1453.

Isberg,R.R. (1991) Discrimination between intracellular uptake and surface adhesion of bacterial pathogens. *Science*, **252**, 934–938.

Isberg,R.R. and Falkow,S. (1985) A single genetic locus encoded by *Yersinia pseudotuberculosis* permits invasion of cultured animal cells by *Escherichia coli* K-12. *Nature*, **317**, 262–264.

Isberg,R.R.and Leong,J.M. (1988) Cultured mammalian cells attach to the invasin protein *Yersinia pseudotuberculosis*. *Proc. Natl Acad. Sci. USA*, **85**, 6682–6686.

Isberg,R.R. and Leong,J.M. (1990) Multiple β1 chain integrins are receptors for invasin, a protein that promotes bacterial penetration into mammalian cells. *Cell*, **60**, 861–871.

Isberg,R.R., Voorhis,D.L. and Falkow,S. (1987) Identification of invasin: a protein that allows enteric bacteria to penetrate cultured mammalian cells. *Cell*, **52**, 769–778.

Jerse,A.E., Yu,J., Tall,B.D. and Kaper,J.B. (1990) A genetic locus of enteropathogenic *Escherichia coli* necessary for the production of attaching and effacing lesions on tissue cells. *Proc. Natl Acad. Sci. USA*, **87**, 7839–7843.

Kornberg,L.J., Earp,H.S., Turner,C.E., Prockop,C. and Juliano,R.L. (1991) Signal transduction by integrins: increased protein tyrosine phosphorylation caused by clustering of β 1 integrins. *Proc. Natl Acad. Sci. USA*, **88**, 8392–8396.

Krukonis,E.S. and Isberg,R.R. (1997) Microbial pathoges and integrin interactions. In Eble,J.A. and Kuehn,K. (eds), *Integrin–Ligand Interaction*. Landes, Austin, TX, pp. 175–197.

Leong,J.M. and Isberg,R.R. (1993) The formation of a disulfide bond is required for efficient integrin binding by invasin. *J. Biol. Chem.*, **268**, 20524–20532.

Leong,J.M., Fournier,R. and Isberg,R.R. (1990) Identification of the integrin binding domain of the *Yersinia pseudotuberculosis* invasion protein. *EMBO J.*, **9**, 1979–1989.

Leong,J.M., Fournier,R. and Isberg,R.R. (1991) Mapping and topographic localization of epitopes of the *Yersinia pseudotubersulosis* invasion protein. *Infect. Immun.*, **59**, 3424–3433.

Leong,J.M., Morrissey,P.E. and Isberg,R.R. (1993) A 76 amino acid disulfide loop in the *Yersinia pseudotuberculosis* invasin protein is required for integrin receptor recognition. *J. Biol. Chem.*, **268**, 20524–20532.

Leong,J.M., Morrissey,P.E., Marra,A. and Isberg,R.R. (1995) An aspartate residue of the *Yersinia pseudotuberculosis* invasin protein that is critical for integrin binding. *EMBO J.*, **14**, 422–431.

Marra,A. and Isberg,R.R. (1997) Invasin-dependent and invasin-independent pathways for translocation of *Yersinia pseudotuberculosis* across the Peyer's patch intestinal epithelium. *Infect. Immun.*, **65**, 3412–3421.

Miller,J., Knorr,R., Ferrone,M., Houdei,R., Carron,C.P. and Dustin,M.L. (1995) Intercellular adhesion molecule-1 dimerization and its consequences for adhesion mediated by lymphocyte function associated-1. *J. Exp. Med.*, **182**, 1231–1241.

Miller,J.H. (1992) *A Short Course in Bacterial Genetics: A Laboratory Manual and Handbook for Escherichia coli and Related Bacteria*. Cold Spring Habor Laboratory Press, Cold Spring Harbor, NewYork.

Miller,V. and Falkow,S. (1988) Evidence for two genetic loci from *Yersinia enterocolitica* that can promote invasion in epithelial cells. *Infect. Immun.*, **56**, 1242–1248.

Miyamoto,S., Akiyama,S.K. and Yamada,K.M. (1995a) Synergistic roles for receptor occupancy and aggregation in integrin transmembrane function. *Science*, **267**, 883–885.

Miyamoto,S., Teramoto,H., Coso,O.A., Gutkind,J.S., Burbelo,P., Akiyama,S.K. and Yamada,K.M. (1995b) Integrin function: molecular hierachies of cytoskeletal and signaling molecules. *J. Cell Biol.*, **131**, 791–805.

Obara,M., Kang,M.S. and Yamada,K.M. (1988) Site-directed mutagenesis of the cell binding domain of human fibronectin: separable, synergistic sites mediate adhesive function *Cell*, **53**, 649–657.

Pepe,J.C. and Miller,V.L. (1990) The *Yersinia enterocolitica inv* gene product is an outer membrane protein that shares epitopes with *Yersinia pseudotuberculosis* invasin. *J. Bacteriol.*, **172**, 3780–3789.

Pepe,J.C., Wachtel,M.R., Wagar,E. and Miller,V.L. (1995) Pathogenesis of defined invasion mutants of *Yersinia enterocolitica* in a Balb/c mouse model of infection. *Infect. Immun.*, **63**, 4837–4848.

Rankin,S., Isberg,R.R. and Leong,J.M. (1992) The integrin-binding domain of invasin is sufficient to allow bacterial entry into mammalian cells. *Infect. Immun.*, **60**, 3909–3912.

Ruoslahti,E. and Pierschbacher,M.D. (1987) New perspectives in cell adhesion: RGD and integrins. *Science*, **238**, 491–497.

Saltman,L.H., Lu,Y., Zaharias,E.M. and Isberg,R.R. (1996) A region of the *Yersinia pseudotuberculosis* invasin protein that contributes to high affinity binding to integrin receptors. *J. Biol. Chem.*, **271**, 23438–23444.

Sambrook,J., Fritsch,E.F. and Maniatis,T. (1989) *Molecular Cloning: A Laboratory Manual*. Cold Spring Harbor Laboratory Press, Cold Spring Harbor, NY.

Schauer,D.B. and Falkow,S. (1993) The *eae* gene of *Citrobacter freundii* biotype 4280 is necessary for colonialization in transmissible murine colonic hyperplasia. *Infect. Immun.*, **61**, 4654–4661.

Simonet,M., Riot,B., Fortineau,N. and Berche,P. (1996) Invasin production by *Yersinia pestis* is abolished by insertion of an IS200-like element within the *inv* gene. *Infect. Immun.*, **64**, 375–379.

Swanson,J.A. and Baer,S.C. (1995) Phagocytosis by zippers and triggers. *Trends Cell Biol.*, **5**, 89–93.

Tran Van Nhieu,G. and Isberg,R.R. (1991) The *Yersinia pseudotuberculosis* invasion protein and human fibronectin bind mutually exclusive sites on the α5β1 integrin receptor. *J. Biol. Chem.*, **266**, 24367–24375.

Tran Van Nhieu,G. and Isberg,R.R. (1993a) Bacterial internalization mediated by β1 chain integrins is determined by ligand affinity and receptor density. *EMBO J.*, **12**, 1887–1895.

Tran Van Nhieu,G. and Isberg,R.R. (1993b) Monoclonal antibodies as ligands promoting integrin-mediated bacterial internalization by cultured cells. *Immunol. Methods*, **2**, 71–77.

Tran Van Nhieu,G., Krukonis,E.S., Reszka,A.A., Horwitz,A.F. and Isberg,R.R. (1996) Mutations in the cytoplasmic domain of the β1 integrin chain indicate a role for endocytosis factors in bacterial internalization. *J. Biol. Chem.*, **271**, 7665–7672.

Van de Water,L., Destree,A.T. and Hynes,R.O. (1983) Fibronectin binds to some bacteria but does not promote their uptake by phagocytic cells. *Science*, **220**, 201–204.

Yang,Y. and Isberg,R.R. (1993) Cellular internalization in the absence of invasin expression is promoted by the *Yersinia pseudotuberculosis yadA* product. *Infect. Immun.*, **61**, 3907–3913.

Young,V.B., Miller,V.L., Falkow,S. and Schoolnik,G.K. (1990) Sequence, localization and function of the invasin protein of *Yersinia enterocolitica*. *Mol. Microbiol.*, **4**, 1119–1128.

Received August 10, 1998; revised December 2, 1998; accepted December 31, 1998